

Direct reactions with radioactive beams

Angela Bonaccorso

INFN, Sezione di Pisa, 56127 Pisa, Italy

E-mail: bonac@df.unipi.it

Abstract. Since the first measurements in the 80's of total reaction cross sections from radioactive beams up to the most recent and advanced exclusive experiments for dripline unbound nuclei, our understanding of exotic nuclei has greatly evolved. This has been possible through a joint effort in the description of the reaction mechanisms and of the underlying nuclear structure. Most exotic nuclei are weakly bound due to the excess of either neutrons or protons and they breakup easily in peripheral reactions. We will discuss in this paper the mechanism responsible for nuclear and Coulomb breakup. Some open problems will be discussed in detail, such as kinematical effects on core parallel momentum distributions and the possibility and consequences that such cores be themselves weakly bound. A general framework for the reaction theory will be used, based on a time dependent perturbation theory approach. Its eikonal limit will be also mentioned.

1. Introduction

There are many reasons to be interested in the physics of exotic nuclei: they can be found in the crust of neutron's stars where they do not β -decay because of the surrounding electrons; by studying them one could hope to answer the fundamental question of nuclear bindings and relative interactions because they extend our understanding of the nuclear force; they help us checking the limits of validity of structure models.

The present state of the art is that we have very sophisticated structure models and extremely complex experiments with relatively "simple" interpretations for the data. "Ab initio" models have started to bridge the gap between structure and reaction theory (see for example Eurisol Lisbon Meeting report on "Physics of Light Exotic Nuclei" [1]). In this panorama one might wonder about which is the rôle of reaction theory and how simple and/or "complicated" does it need to be. In the following I shall try to show that first of all reaction theory helps understanding the reaction mechanisms. Then it provides guidance in the search for the best *observable* to be measured, in view of the reduced intensity of RIBs. Finally I will discuss the accuracy of methods and numerical implementations.

2. Early experiments and theory

A new chapter in the history of studies of nuclear reactions started around 1985 with the seminal papers by Tanihata *et al.* [2, 3]. Interaction cross sections, defined as the total reaction cross sections for the change of proton and/or neutron number in the incident nucleus were reported for a series of light nuclei. The measurements had been done at the Bevalac of the Lawrence Laboratory in Berkeley for a series of light nuclei at 790A.MeV on light targets. The systematic showed very large cross sections for some of them. Tanihata *et al.* in view of the high incident



energies involved, used a simple geometrical model to interpret the data and deduced unexpected large interaction radii. Some of the "unusual" nuclei were: ^6He , ^{11}Be , ^{11}Li , ^{14}Be . Besides the importance of the unexpected results these papers were the first to show that beams of unstable nuclei could be used for nuclear structure studies. A detailed account of subsequent developments can be found in Ref. [4]. Very narrow parallel momentum distributions were also a simple and clear observable measured in the spectrometers [5]-[7]. It was soon clear that the anomalous behavior was due to one or two very weakly bound neutrons whose breakup was dominating the interaction cross section. Interestingly it took twenty five more years to see very clearly such effects in the elastic scattering of ^{11}Be [8].

One and/or two nucleon breakup cross sections from ^{11}Be , ^{11}Li were measured in some pioneering experiments, and discussed in the Anne *et al.* papers [9]. Neutron angular distributions following breakup on three targets of increasing mass were measured. They allowed to distinguish the nuclear and Coulomb breakup mechanisms. At the same time some coincidence experiments [10] with neutrons decaying from excited states of an heavy target gave evidence for the presence of possible projectile-target inelastic excitations associated with breakup along not too peripheral trajectories. These effects were associated with long tails of the core parallel momentum distributions. Up-to-date this interesting phenomenon seen very often on momentum distributions has not been clarified. More recently possible effects of core excitations have been seen and discussed in Refs. [11, 12].

While experiments were planned and performed at various facilities in the world the first theoretical interpretations of the early data started to appear. Hansen and Jonson [13] were the first to propose the presence of a neutron halo as responsible for the large interaction cross sections and narrow momentum distributions. Other works followed, see for example [14, 15] in which the origin of the halo was attributed to the shell inversion between $2s$ and $1p_{1/2}$ states caused by core excitations.

3. Interaction cross sections and halo decoupling from the core

As mentioned above Tanihata *et al.* in view of the high incident energies involved, used a simple geometrical model to interpret their first data on interaction cross sections and deduced unexpected large interaction radii. The hypothesis was that projectile and target would not overlap such that $\sigma_R = \pi(R_p^I + R_t^I)^2$. Later on the Glauber model was introduced

$$\sigma_R = \int_0^\infty d\mathbf{b}(1 - |S_{NN}(\mathbf{b})|^2) = \sigma_{ct} + \sigma_{nt} \quad (1)$$

where for the first time the decoupling of core and valence particle, later on identified as "halo" [13], was explicitly considered. It was obtained by first introducing the optical limit of Glauber theory for the phase shift and then writing the total density of the halo nucleus as a sum of the core and valence particle densities, such that

$$|S_{NN}(\mathbf{b})|^2 = e^{-[\sigma_{nn} \int ds \rho_p(|\mathbf{b}-\mathbf{s}|) \rho_t(\mathbf{s})]} = e^{-[\sigma_{nn} \int ds \rho_c \rho_t]} e^{-[\sigma_{nn} \int ds \rho_n \rho_t]}. \quad (2)$$

Equation (2) can be obtained only if $\rho_p = \rho_c + \rho_n$. Such a decoupling of core and valence particle is justified if ρ_c and ρ_n can be considered to span different regions of the projectile-target distance $|\mathbf{b} - \mathbf{s}|$. Thus ρ_n must represent only the peripheral part of the bound state wave function with no significant contribution from the internal region where the particle is in the same potential as the core nucleons. For a true halo this condition is always satisfied. For normally bound nuclei instead some caution has to be taken.

The second factor in equation (2) contains the neutron-target phase shift in the exponent $|S_{nt}|^2 = e^{-[\sigma_{nn} \int ds \rho_n \rho_t]}$. If it can be considered small, then to first order

$$|S_{NN}(\mathbf{b})|^2 = |S_{ct}|^2 |S_{nt}|^2 = |S_{ct}|^2 - |S_{ct}|^2 [\sigma_{nn} \int ds \rho_n \rho_t]. \quad (3)$$

Substitution of this expression in equation (1) leads to the sum of core-target and neutron-target cross sections.

In most halo nuclei there are no bound excited states, therefore the second term in equation (3) was interpreted as the halo breakup probability $P_{bup}(\mathbf{b}_c) \approx \sigma_{nn} \int ds \rho_n \rho_t$ such that one finally obtains

$$\sigma_{nt} = \int_0^\infty d\mathbf{b}_c |S_{ct}(\mathbf{b}_c)|^2 P_{bup}(\mathbf{b}_c). \quad (4)$$

Here the no-recoil approximation has been used leading to the substitution of the projectile-target impact parameter \mathbf{b} with the core-target impact parameter \mathbf{b}_c . Equations (3)-(4) constituted the building blocks of all subsequent models of halo breakup. In particular equation (4) shows clearly that the condition that the core will be detected intact is of fundamental importance for a correct treatment of breakup and is represented theoretically by $|S_{ct}|^2$. However it was soon realized that the expression for the halo breakup P_{bup} given above was not accurate as it contained the neutron-target interaction only to first order. In the following we shall use more accurate expressions for all breakup cross section calculations, in which an all order treatment of the neutron-target interaction will be used. Recent reports on the experimental and theoretical situation up-to-date can be found in the volume [16].

4. Parallel momentum distributions from breakup

At the early stages of the use of RIBs, besides the interaction cross sections, parallel momentum distributions of the cores following one nucleon breakup, were measured by Tanihata, Kobayashi and collaborators [5] and soon after by several other groups at various facilities [17]-[29]. Based on previous theoretical work [30]-[35] on normal nuclei, it was soon clear that such distributions represented a somewhat distorted "photography" of the Fourier transform of the initial state wave function, and thus could represent a useful way to perform systematic spectroscopic studies of exotic nuclei. The theoretical seminal papers in this field were Refs. [36]-[40]. Following some early publications concentrated on understanding the reaction dynamics correctly to quantify the amount of "distortion" due to the reaction mechanism both experimentally [7] and theoretically [41], an intense activity devoted to spectroscopic studies started with Hansen and collaborators [20] using systematic measurements of parallel momentum distribution and total breakup cross sections to deduce the angular momenta of the initial states and the spectroscopic factors which would make the link between data and the shell model description of exotic nuclei.

The breakup probability in equation (4) which is the sum of the elastic breakup and a second contribution called inelastic breakup or stripping can be obtained if the closure approximation is used [37] in an "all order" eikonal model more refined than in equation (3). This is possible if the nuclei under study do not have bound excited states. Thus the total breakup probability reads

$$P_{-n}(\mathbf{b}_c, k_1) = \int_0^\infty d\mathbf{b}_v (|1 - S(\mathbf{b}_v)|^2 + 1 - |S(\mathbf{b}_v)|^2) |\tilde{\psi}_i(|\mathbf{b}_v - \mathbf{b}_c|, k_1)|^2 \quad (5)$$

where $S(\mathbf{b}_v)$ is the valence nucleon-target S-matrix. $\tilde{\psi}_i$ is the one dimensional Fourier transform of the initial state wave function of the breakup nucleon. $k_1 = (\varepsilon_f - \varepsilon_i - \frac{1}{2}mv^2)/(\hbar v)$, is the neutron (proton) parallel momentum component with respect to the core. Also ε_i is the initial binding energy of the valence particle in the projectile and ε_f its final energy with respect to the target. $\frac{1}{2}mv^2$ is the incident energy per particle at the distance of closest approach. By energy and momentum conservation the core parallel momentum distribution in the laboratory is given by:

$$P_{//} = \sqrt{(T_p + \varepsilon_i - \varepsilon_f)^2 + 2M_r(T_p + \varepsilon_i - \varepsilon_f)}, \quad (6)$$

such that a measure of the latter is considered to give a direct information on the momentum distribution of the valence particle in the initial state of the projectile. Thus inserting equation (5) in equation (4) the cross section differential with respect to the intrinsic parallel momentum in the core is obtained. By using equation (6) and the relative jacobian the cross sections becomes directly comparable to the measured momentum distributions.

Here $P_{//}$ is given in terms of the projectile kinetic energy T_p and of the residual nucleus (A_p-1) mass M_r . Indicating by $M_{p,t,n}$ the projectile, target and neutron mass respectively, then equation (6) is obtained by applying first energy conservation between initial and final states

$$M_p + T_p + M_t = T_r + M_r + M_n + M_t + \varepsilon_f, \quad (7)$$

if the target mass is conserved ($\varepsilon_f \ll M_t$), M_t cancels out and

$$T_r = T_p + M_p - (M_r + M_n) - \varepsilon_f = T_p + \varepsilon_i - \varepsilon_f \quad (8)$$

where $-\varepsilon_i \equiv (M_r + M_n) - M_p$ is by definition, the valence neutron separation energy in the projectile. Under the eikonal hypothesis that energy is converted mainly in parallel momentum, inserting (8) in $P_{//} = \sqrt{(T_r + M_r)^2 - M_r^2}$ then equation (6) readily follows.

In this way some kinematical constraints can be satisfied even if an eikonal formalism is used without the need to take the sudden limit [30, 42]. However if the incident energy is very high and the initial separation energy very small, then one can extend the limit of k_1 from $-\infty \rightarrow +\infty$. Integrating back on k_1 the momentum distribution the total breakup cross section reads

$$\sigma_{nt} = \Sigma_i (C^2 S)_i \int_0^\infty d\mathbf{b}_c d\mathbf{b}_v |S_{ct}(\mathbf{b}_c)|^2 (|1 - S(\mathbf{b}_v)|^2 + 1 - |S(\mathbf{b}_v)|^2) |\psi_i(|\mathbf{b}_v - \mathbf{b}_c|)|^2. \quad (9)$$

This equation is consistent with equation (4.17) of [33], and we have considered that if different initial states contribute to the inclusive breakup cross section (see section IV of Ref. [43]) their contribution should be summed both in the spectra as well as in the integrated cross sections, each weighted by the relative initial wave function spectroscopic factor C^2S . This method has been largely followed in the past years after the seminal applications presented in [20]. Spectroscopic factors have been extracted from the ratio of measured and calculated total breakup cross sections while the angular momentum of the initial state has been deduced from the shape of the momentum distribution. Such approaches derive from the use of shell model initial state wave functions. Recently ab-initio wave functions have also been used [24].

5. Kinematical effects on breakup

The breakup models discussed in section 2 were introduced having in mind very high incident energies and small initial state separation energies. Under such conditions energy and momentum conservation can be neglected. However some dynamical effects are always present [35] and become very important when the separation energies are large and the incident energies comparable to them. This has recently been verified in relation to studies of exotic nuclei having large differences in the proton-neutron separation energies ($\Delta S = |S_n - S_p| \approx 20\text{MeV}$) [11]. Such situations are more accurately described in a time dependent formalism. Starting again from equation (4) if the breakup probability is calculated in the target reference frame, then the initial state wave function has to be boosted by a Galilean transformation following which the time dependent exponentials become $e^{-ik_1 z'} e^{ik_2 z}$ where k_1 , which has already been defined, and $k_2 = (\varepsilon_f - \varepsilon_i + \frac{1}{2}mv^2)/(\hbar v)$ are the z-components of the neutron momentum in the initial and final state respectively. $\eta^2 = k_1^2 + \gamma_i^2 = k_2^2 - k_f^2$ is the magnitude of the transverse component

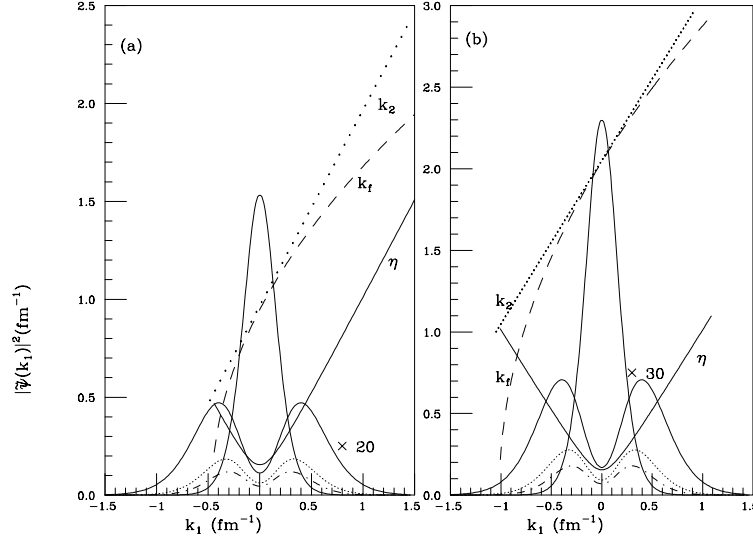


Figure 1. Initial state momentum distributions [35], as a function of k_1 . For an s-state full curve peaked at $k_1 = 0$. For a d-state: dtdashed, dotted and thin solid curves. The dotted line is k_2 , the dashed line is k_f , and the solid line is η , see text for definitions. (a) $T_p/A_p = 20\text{MeV}$, (b) $T_p/A_p = 88\text{MeV}$.

$k_\perp = i\hbar\eta$ of the neutron momentum in the initial and final state. Here $\gamma_i = \sqrt{-2m\varepsilon_i}/\hbar$, $k_f = \sqrt{2m\varepsilon_f}/\hbar$ and k_\perp is conserved during the breakup process and it is purely imaginary because the neutron which in the initial state has negative energy [44] is emitted through a potential barrier. Because of this it holds also $k_2 > k_f$. It is straightforward to see from the definitions of these kinematical variables that they satisfy the neutron energy and momentum conservation. In this time dependent formalism that we call transfer-to-the-continuum (TC) [35][41]-[43] [45]-[47], the breakup probability reads

$$\frac{dP}{dk_1} \approx \frac{1}{2} \sum_{j_f} (|1 - \bar{S}_{j_f}|^2 + 1 - |\bar{S}_{j_f}|^2) (2j_f + 1) (1 + R) \left[\frac{\hbar}{mv} \right] \frac{1}{k_f} |C_i|^2 \frac{e^{-2\eta b_c}}{2\eta b_c} M_{l_f l_i}. \quad (10)$$

\bar{S}_{j_f} are neutron-target S-matrices calculated according to the optical model, including the spin-orbit term of the neutron-target optical potential. The sum over partial waves in equation (10) is indeed a sum over total neutron-target angular momenta. C_i are the initial wave function asymptotic normalization constant. The form factor $\frac{e^{-2\eta b_c}}{2\eta b_c}$ is due to the combined effects of the initial and final wave function Fourier transforms, while $M_{l_f l_i}$ is due to the overlap of the angular parts. Detailed definitions can be found in Ref. [35].

Under the sudden (or adiabatic) hypothesis the parallel momentum distribution of the neutron in the projectile is frozen during the reaction and its shape should be reflected by the final measured distribution. The available neutron final energy is all converted into parallel

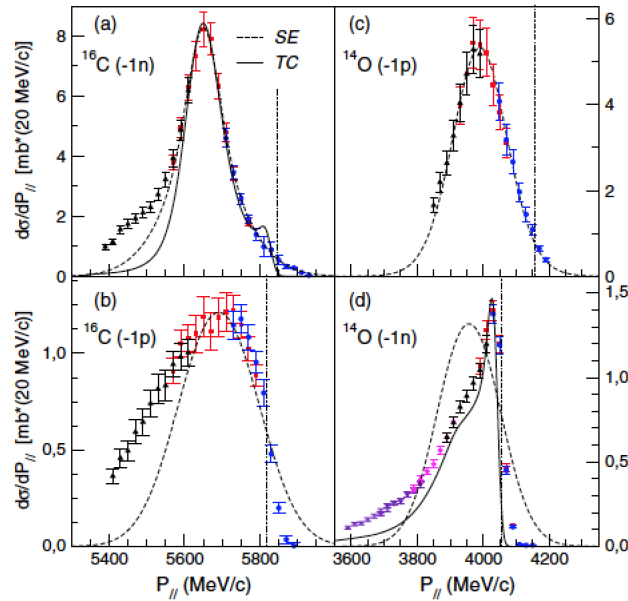


Figure 2. (Color online) Examples of spectra from Refs. [11].

momentum. Interference effects with the transverse distribution are in this way neglected. The sudden hypothesis means also that the whole momentum distribution in the initial state is sampled during the reaction, while the correct kinematical conditions, expressed in the definition of k_1 and k_2 , constrain the phase space sampled by the reaction. Also, in the present approach in order to realize the best energy matching conditions for each possible final energy ε_f of the neutron, the reaction mechanism shares the total momentum k_f between the transverse momentum component η and the parallel component k_2 , thus allowing the interference (cf. also equation (3) of [41]) between the two corresponding distributions. The factor $M_{l_f l_i}$ in equation (10) contains the interference effects. Thus measured parallel momentum distribution might look deformed as compared to the parallel momentum distribution of the neutron in the initial state.

In order to clarify the importance of the energy sharing between the parallel and transverse components of the neutron final momentum, we show in figures 1a and 1b [35], corresponding to an incident energy of 20A.MeV and 88A.MeV, respectively, the following kinematical variables as functions of k_1 , the neutron initial momentum with respect to the projectile: k_2 , the neutron final parallel momentum component with respect to the target, by the dotted line; k_f , the magnitude of the total neutron momentum corresponding to each neutron final continuum energy ε_f , by the dashed line; η the neutron transverse momentum component, by the solid line. The minimum values of k_1 correspond to $\varepsilon_f = 0$. Values of all parameters corresponding to values of $\varepsilon_f < 0$ are not accessible by breakup reactions but they would rather correspond to transfer to a final bound state. In both figures there is a region corresponding to very small values of η in which $k_2 \approx k_f$. This is the region of validity of the sudden eikonal approximation. In fact in such conditions since the transverse component of the neutron momentum η is very small, the total momentum k_f is all converted into parallel momentum k_2 . In [41] we showed indeed that the condition $k_2 \approx k_f$ was necessary to obtain the eikonal form of the breakup amplitude. In the same figures we show the initial s and d distributions of the parallel neutron momentum as a function of k_1 . The shapes of such distributions depend critically from the initial single particle wave function angular momentum through the angular part of the wave function and then of the

momentum distribution. That one neutron breakup could be used to measure such distributions was first suggested in Ref. [45] where normal nuclei were studied.

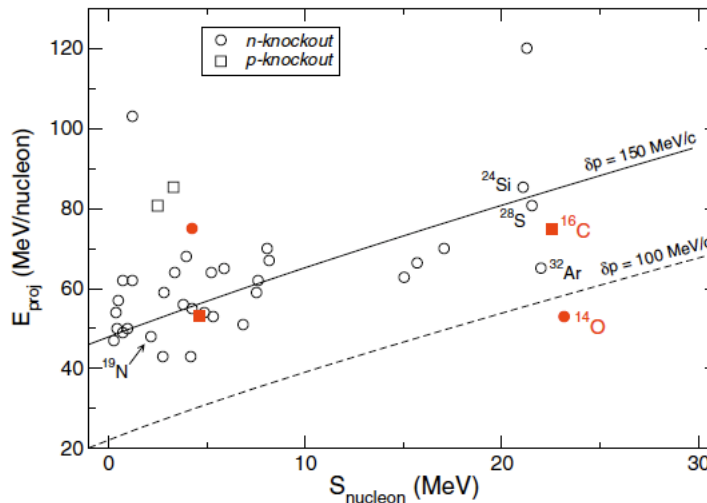


Figure 3. (Color online) Kinematic relation between the energy per nucleon of the projectile and the separation energy of the removed nucleon for a given position of the cutoff. The lines correspond to cutoffs appearing at $\delta p = 100$ and 150 MeV/c with respect to the center of the "sudden" distribution. Data points are taken from [22, 23, 24]. Data points from [11] are indicated with filled (red) symbols.

The initial distributions get wider by increasing the absolute value of the initial binding. Therefore the eikonal approximation is best justified in a range of $k_1 \approx 0$ values and for initial distributions, like the $l_i = 0$ one, concentrated in such a region. Figure 1b shows that such a range increases by increasing the incident energy. On the other hand figure 1a shows that at incident energies around 20A.MeV an important part of the initial neutron momentum distribution corresponding to k_1 values from $-\infty$ to about -0.5 fm^{-1} would not be kinematically allowed. Thus using the frozen limit would give too wide momentum distributions and too large breakup cross sections.

The kinematical effects discussed in this section have recently been seen clearly in some experimental data [11] that we show in figure 2 (d-quadrant). The core parallel momentum spectrum following $^{14}\text{O} + ^9\text{Be}$ one neutron breakup at 53A.MeV is shown. Note that in this case the neutron initial separation energy is $S_n = 23.2 \text{ MeV}$. As expected the spectrum is very deformed and shows a cutoff consistent with equation (6). Furthermore in figure 3 we show the amount of cutoff affecting a series of recent data as a function of initial incident energy and separation energy. δp is easily understood by looking at figure 1 as the absolute value of the lower kinematically allowed limit of k_1 in MeV/c. Such results were already predicted in Ref. [42].

6. Coulomb dissociation and proton breakup

When the target is heavy the effect of the core-recoil, due to the Coulomb interaction between projectile and target, gives rises to a further source of breakup. The dipole approximation for the Coulomb potential is the standard approximation to calculate neutron halo "Coulomb dissociation" as it gives correctly the core-recoil mechanism which causes the reaction [48, 49]. However it is not applicable when the valence particle is a proton. This is due to the fact that

in proton breakup there is a very important direct Coulomb proton-target term which needs to be treated correctly, to all orders and all multiplicities as it has been made clear in several publications [50]-[55]. We remind the reader that in calculating breakup, to treat an interaction to all orders means to have in the probability amplitude a final wave function which takes into account all final state interactions of the breakup particle with the target. This is well achieved with the eikonal wave function, as it is easily seen if one expands in series the phase shift. On the other hand to treat the interaction to all multiplicities means that either no multipole expansion is done or all terms are taken into account. The extension of our formalism to take into account the full Coulomb potential for a neutron breakup was made in Ref. [53], while the proton breakup formalism was first introduced in Ref. [54] and then studied in detail in Ref. [55].

The Coulomb potential responsible for proton breakup is

$$V(\mathbf{r}, \mathbf{R}) = \frac{V_c}{|\mathbf{R} - \beta_1 \mathbf{r}|} + \frac{V_v}{|\mathbf{R} + \beta_2 \mathbf{r}|} - \frac{V_0}{R} \quad (11)$$

where $V_c = Z_c Z_t e^2$, $V_v = Z_v Z_t e^2$ and $V_0 = (Z_v + Z_c) Z_t e^2$. β_1 and β_2 are the mass ratios of proton and core, respectively, to that of the projectile. Z_c , Z_t and Z_v are the core, target and proton charge respectively. In this case the differential cross section will get contribution from three terms such that it reads:

$$\frac{d\sigma}{d\mathbf{k}} = \frac{1}{8\pi^3} \int d\mathbf{b}_c |S_{ct}(\mathbf{b}_c)|^2 |g^{rec} + g^{dir} + g^{nuc}|^2, \quad (12)$$

where \mathbf{k} is the proton final momentum in the continuum and the density of final states has been introduced. See Ref. [55] for further notation details.

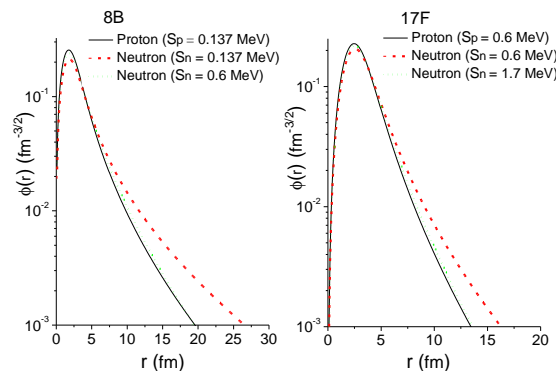


Figure 4. (Color online) Proton vs neutron wave functions for a $p_{3/2}$ single particle state in a ^8B and $d_{5/2}$ in ^{17}F as indicated.

In Ref. [55] we followed an idea already presented in Ref. [56] and tried to understand proton breakup in terms of the well known characteristics of neutron breakup. We found that from the point of view of the nuclear breakup a proton behaves exactly as a neutron having an "effective" binding energy

$$\tilde{\varepsilon}_i = \varepsilon_i - \Delta = \varepsilon_i - \frac{Z_p e^2}{R_i} - Z_t e^2 \left(\frac{1}{2} \left(\frac{1}{|b_c + \beta_2 R_i|} + \frac{1}{|b_c - \beta_1 R_i|} \right) - \frac{1}{b_c} \right), \quad (13)$$

which through the factors β_1 and β_2 is consistent with equation (11). R_i the position of the projectile top of the Coulomb barrier, b_c is the distance between the center of the two nuclei for which the top of the two Coulomb barriers of projectile and target coincide.

We checked this idea by fitting wave functions for a neutron and a proton in a Woods-Saxon potential. Figure 4 shows two cases for ^8B and ^{17}F from Ref. [55]. By applying this method we were able to understand that from the point of view of the nuclear breakup a proton behaves exactly as a neutron of larger binding energy. Our prescription for the effective energy equation (13) proved to be quite accurate but as expected the effective separation energy has to be "incident energy dependent". This is because it contains an average estimate of the Coulomb barrier effect at a fixed typical distance between projectile and target. Such distance is expected to be incident-energy dependent. Indeed the results of Ref. [57] where CDCC calculations were performed for $^{17}\text{F}+^{208}\text{Pb}$ at 170MeV, show that at lower incident energies the effective binding energy increases.

On the other hand the Coulomb breakup is dominated by the direct proton-target interaction, as it can be seen from the figures and discussions in Refs. [55] where we showed the utility of using the breakup proton angular distributions to disentangle the reaction mechanism. We finish this section by suggesting that proton halo candidates should be investigated via nuclear breakup and compared to neutron breakup at high incident energy where the effects of the reaction mechanisms will be minimal.

7. Breaking a strongly bound neutron but skipping a weakly bound proton

Table 1. One-nucleon knockout results from ^{14}O on ^9Be at 53 A.MeV. Calculated inclusive cross sections σ_{TC} from the TC approach are shown and compared to the measured (σ_{exp}) cross sections. Theoretical spectroscopic factors C^2S from [11]. Reduction factors are indicated and defined as R_f in order to distinguish from the strong absorption radius notation (R_s).

Residue	$S_{p(n)}$ (MeV)	J^π	σ_{exp} (mb)	C^2S	σ_{sp} (mb)	σ_{sp}^{nop} (mb)	σ_{TC} (mb)	σ_{TC}^{nop} (mb)	R_f
^{13}N	4.6	$1/2^-$	58(4)	1.83	34.2		53		0.9
^{13}O	23.1	$3/2^-$	14(1)	3.15	10.9	8.6	34.5	27.1	0.5

There are situations in which a strongly bound neutron is knocked out but a weakly bound proton in the same projectile is not. The final cross section formula for a reaction of this type must contain some information on the strong reaction channel that one thinks is suppressed, thus we suggest the following correction:

$$\sigma_{TC}^{nop} = C^2S \int_0^\infty d\mathbf{b}_c P_{-n}(b_c) e^{-P_{-p}} |S_{ct}(b_c)|^2,$$

where $e^{-P_{-p}} \approx 1 - P_{-p}(b_c)$, is the probability than the weakly bound particle in the projectile does not breakup. This is equivalent to calculating a Dynamic Polarization Potential (DPP) from phase shift following [58]

$$|S_{NN}(b_c)|^2 = e^{-4\delta_I(b_c)} = e^{-4\delta_I^V(b_c)} e^{-4\delta_I^S(b_c)} = |S_{ct}(b_c)|^2 e^{-P_{-p}(b_c)}.$$

This improved formalism has been applied to the reaction previously studied in Refs. [11, 59]. Using the Dispersive Optical Potential neutron-target S-matrices of Ref. [60] we obtained the

results shown in table 1. The single particle neutron/proton wave functions were calculated in the Woods-Saxon potential given in Ref. [59]. The proton wave function was calculated according to Ref. [55], as a neutron wave function having an effective binding energy such as to fit the exact proton wave function of Ref. [59]. The results of table 1 for the reduction seen in the spectroscopic factors are consistent with those of Ref. [59] which makes one thinking that transfer and knockout lead to the same results about reduction factors if almost all uncertainties due to the difference in wave functions (structure information) are removed and if the weakly and strongly bound particle breakup are treated consistently, including kinematical cutoff and the effect of the DPP on the core.

8. Conclusions

In this contribution I have discussed some direct reactions used to study exotic nuclei and I have tried to enlighten open problems for the future. My final remarks are as follows. From simple halo nucleus beams we have gone to more complicated RIBs, therefore reaction theory needs to accommodate such developments and simple eikonal models of knockout need to be improved by including kinematics and a better treatment of the core-target scattering in particular when strong reaction channels such as breakup would be expected for the core. From the experimental point of view, kinematical complete experiments are necessary with reconstruction of the target final state and core angular distributions if and when possible. It would be nice to have more proton breakup experiments since we now understand better the dynamics of their reactions. The past has been characterized by studies at high incident energy and for weakly bound projectiles. In the future more and more strongly bound nuclei will be studied at lower energies at ISOL-type facilities. Then the issues raised here will be particularly relevant.

Acknowledgements

Some unpublished results presented in this paper have been obtained in collaboration with Charity R J, Flavigny F, Obertelli A and Salvioni G. I thank Barbieri C for providing his overlap functions.

References

- [1] http://www.df.unipi.it/~angela/lisbon_report.pdf
- [2] Tanihata I *et al.* 1985 *Phys. Lett. B* **160** 380
- [3] Tanihata I *et al.* 1985 *Phys. Rev. Lett.* **55** 2676
- [4] Tanihata I 1995 *Prog. Part. Nucl. Phys.* **35** 505
- [5] Kobayashi T *et al.* 1988 *Phys. Rev. Lett.* **60** 2599
- [6] Tanihata I 2011 *Nucl. Phys. A* **685** 80c
- [7] Kelley J H *et al.* 1995 *Phys. Rev. Lett.* **74** 30
- [8] Di Pietro A *et al.* 2010 *Phys. Rev. Lett.* **105** 22701
- [9] Anne R *et al.* 1990 *Phys. Lett. B* **250** 19; 1993 *Phys. Lett. B* **304** 55; 1994 *Nucl. Phys. A* **575** 125
- [10] P  rier Y *et al.* 1999 *Phys. Lett. B* **459** 55
- [11] Flavigny F *et al.* 2012 *Phys. Rev. Lett.* **108** 252501
- [12] Louchart C *et al.* 2011 *Phys. Rev. C* **83** 011601
- [13] Hansen P G and Jonson B 1997 *Euro Phys. Lett.* **4** 409
- [14] Zhukov M V *et al.* 1993 *Phys. Rep.* **231** 151
- [15] Vinh Mau N 1995 *Nucl. Phys. A* **592** 33
- [16] Proceedings Nobel Symposium NS152, Fahlander C, Jonson B eds 2013 *Phys. Scr. T* **152** 1
- [17] Orr N *et al.* 1992 *Phys. Rev. Lett.* **69** 2050
- [18] Blank B *et al.* 1991 *Z. Phys. A* **340** 41
- [19] Kobayashi T *et al.* 1989 *Phys. Lett. B* **232** 51
- [20] Hansen P G and Tostevin J A 2003 *Ann. Rev. Nucl. Part. Sci.* **53** 219
- [21] Riisager H *et al.* 1992 *Nucl. Phys. A* **540** 365
- [22] Sauvan E *et al.* 2000 *Phys. Lett. B* **491** 1
- [23] Gade A *et al.* 2008 *Phys. Rev. C* **77** 044306

- [24] Grinyer G *et al.* 2011 *Phys. Rev. Lett.* **106** 162502; 2012 *Phys. Rev. C* **86** 024315
- [25] Hansen P G, Jensen A S, and Jonson B 1995 *Ann. Rev. Nucl. Part. Sci.* **45** 591
- [26] Schwab W *et al.* 1995 *Z. Phys. A* **350** 238
- [27] Pecina I *et al.* 1995 *Phys. Rev. C* **52** 191
- [28] Negoita F *et al.* 1996 *Phys. Rev. C* **54** 1787
- [29] Bazin D *et al.* 1995 *Phys. Rev. Lett.* **74** 3569; 1998 *Phys. Rev. C* **57** 2156
- [30] Bonaccorso A and Brink D M 1998 *Phys. Rev. C* **58** 2864
- [31] Serber R 1947 *Phys. Rev.* **72** 1008
- [32] Baur G, Rösler F, Trautmann D, and Shyam R 1984 *Phys. Rep.* **111** 33
- [33] Hussein M S and McVoy K W 1985 *Nucl. Phys. A* **445** 124
- [34] Bertulani C A and Hussein M S 1990 *Phys. Rev. Lett.* **64** 1099
- [35] Bonaccorso A 1999 *Phys. Rev. C* **60** 054604; 1999 *Nucl. Phys. A* **649** 315c
- [36] Bertsch G F, B. A. Brown, and Sagawa H 1989 *Phys. Rev. C* **39** 1154
- [37] Yabana K, Ogawa Y, and Suzuki Y 1992 *Nucl. Phys. A* **539** 295; 1992 *Phys. Rev. C* **45** 2909
- [38] Bertulani C A and McVoy K W 1992 *Phys. Rev. C* **46** 2638
- [39] Sagawa H and Takigawa N 1994 *Phys. Rev. C* **50** 985
- [40] Hencken K, Bertsch G F, and Esbensen H 1996 *Phys. Rev. C* **54** 3043
- [41] Bonaccorso A and Brink D M 1998 *Phys. Rev. C* **57** R22
- [42] Bonaccorso A and Bertsch G F 2001 *Phys. Rev. C* **63** 044604
- [43] Bonaccorso A and Brink D M 1994 *Phys. Rev. C* **49** 329
- [44] Bonaccorso A, Brink D M, and Lo Monaco L 1987 *J. Phys. G* **13** 1407
- [45] Bonaccorso A and Brink D M 1991 *Phys. Rev. C* **44** 1559
- [46] Bonaccorso A and Brink D M 1988 *Phys. Rev. C* **38** 1776
- [47] Bonaccorso A and Brink D M 1991 *Phys. Rev. C* **43** 299
- [48] Margueron J, Bonaccorso A, and Brink D M 2002 *Nucl. Phys. A* **703** 105
- [49] Margueron J, Bonaccorso A, and Brink D M 2003 *Nucl. Phys. A* **720** 337
- [50] Esbensen H, Bertsch G F, and Bertulani C A 1995 *Nucl. Phys. A* **581** 107
- [51] Esbensen H and Bertsch G F 2002 *Phys. Rev. C* **66** 044609
- [52] Esbensen H, Bertsch G F, and Snover K A 2005 *Phys. Rev. Lett.* **94** 042502
- [53] García-Camacho A, Bonaccorso A, and Brink D M 2006 *Nucl. Phys. A* **776** 118
- [54] García-Camacho A, Blanchon G, Bonaccorso A, and Brink D M 2007 *Phys. Rev. C* **76** 014607
- [55] Ravinder Kumar and Bonaccorso A 2011 *Phys. Rev. C* **84** 014613; 2012 *Phys. Rev. C* **86** 061601(R)
- [56] Bonaccorso A, Brink D M, and Bertulani C A 2004 *Phys. Rev. C* **69** 024615
- [57] Kucuk Y and Moro A M 2012 *Phys. Rev. C* **86** 034601
- [58] Bonaccorso A and Carstoiu F 2002 *Nucl. Phys. A* **706** 322
- [59] Flavigny F *et al.* 2013 *Phys. Rev. Lett.* **110** 122503
- [60] Bonaccorso A and Charity R J 2014 *Phys. Rev. C* **89** 024619